Structure and transport of aqueous electrolytes: From simple halides to radionuclide ions

Remco Hartkamp and Benoit Coasne

Citation: The Journal of Chemical Physics **141**, 124508 (2014); doi: 10.1063/1.4896380
View online: http://dx.doi.org/10.1063/1.4896380
View Table of Contents: http://scitation.aip.org/content/aip/journal/jcp/141/12?ver=pdfcov
Published by the AIP Publishing

Structure and transport of aqueous electrolytes: From simple halides to radionuclide ions

Remco Hartkamp[1,2,a)] and Benoit Coasne[1,2,b)]
[1]*Institut Charles Gerhardt Montpellier, CNRS (UMR 5253), Université Montpellier 2, ENSCM, 8 rue de l'Ecole Normale, 34296 Montpellier Cedex 05, France*
[2]*MultiScale Material Science for Energy and Environment, CNRS/MIT (UMI 3466), Department of Civil and Environmental Engineering, Massachusetts Institute of Technology, 77 Massachusetts Avenue, Cambridge, Massachusetts 02139, USA*

(Received 27 June 2014; accepted 12 September 2014; published online 29 September 2014)

Molecular simulations are used to compare the structure and dynamics of conventional and radioactive aqueous electrolytes: chloride solutions with sodium, potassium, cesium, calcium, and strontium. The study of Cs^+ and Sr^{2+} is important because these radioactive ions can be extremely harmful and are often confused by living organisms for K^+ and Ca^{2+}, respectively. Na^+, Ca^{2+}, and Sr^{2+} are strongly bonded to their hydration shell because of their large charge density. We find that the water molecules in the first hydration shell around Na^+ form hydrogen bonds between each other, whereas molecules in the first hydration shell around Ca^{2+} and Sr^{2+} predominantly form hydrogen bonds with water molecules in the second shell. In contrast to these three ions, K^+ and Cs^+ have low charge densities so that they are weakly bonded to their hydration shell. Overall, the structural differences between Ca^{2+} and Sr^{2+} are small, but the difference between their coordination numbers relative to their surface areas could potentially be used to separate these ions. Moreover, the different decays of the velocity-autocorrelation functions corresponding to these ions indicates that the difference in mass could be used to separate these cations. In this work, we also propose a new definition of the pairing time that is easy to calculate and of physical significance regardless of the problem at hand. [http://dx.doi.org/10.1063/1.4896380]

I. INTRODUCTION

Interactions between ions and water are omnipresent; the presence of ions alters the structure and dynamics of the solvent and contributes to countless biological, chemical, and physical processes. Electrolytes partially or fully dissociate when they are dissolved in water. The dissociation of electrolyte does not only happen when brought into contact with water, ion pairs form and break constantly. In order to form or break an ion pair the structure of the water molecules around the hydrated ions need to be disturbed.[1] This process is perpetuated by the constant competition between electrostatic forces, dispersion forces, and hydrogen bonds.

The solvent structure around hydrated ions, which mainly depends on the ion size and charge, determines for a great part the affinity of two ions of opposite charge to associate or dissociate. Lee[2] showed that the solubility of monovalent electrolytes in water is the smallest (thus most associated cation-anion pairs) if the cation and anion are size-symmetric. Collins[3] further discussed the topic of ion pairing in terms of kosmotropes and chaotropes: kosmotropes are monovalent ions that bind stronger to nearby water than water binds to itself, while chaotropes are monovalent ions that have a weaker binding strength with nearby water molecules. Collins added kosmotrope-kosmotrope interaction to this ordering as the strongest binding strength and chaotrope-chaotrope interactions as the weakest. Thus the pairing affinity and the hydration structure of a solvated ion depends on the cations as well as the anions. Furthermore, these structural properties can depend on ion concentration.[4] For highly concentrated solutions the classification of kosmotropes and chaotropes has been challenged,[5] while for lower ion concentrations these concepts have been widely accepted.[6,7] The model of Collins was recently further investigated by Fennell *et al.*[1] The authors calculated the association constant and the potential of mean force for a single ion-ion pair in water. They concluded that the interaction between kosmotropes is large due to strong electrostatic interaction. On the other hand, the electrostatic interaction between two chaotropes is weak, but these ions are held together by a water cage around the ion pair. A kosmotrope-chaotrope pair immediately dissociates because the ionic binding and the water-water binding are both weaker than the interaction between the kosmotrope and nearby water molecules.

A study of the dynamics of ions and water molecules can complement the understanding obtained from structural quantities. Notable studies of ion-water residence times include the pioneering work of Impey *et al.*[8] These authors defined a mean residence time (MRT) by assuming an exponentially decaying correlation of the survival probability of a pair; the residence time is then equal to the decay rate of the correlation function. This work has paved the way for many more studies on residence of water near an ion,[9] but also ion-ion pairing,[10] dynamics of hydrogen bonds,[11] ion residence in a confined fluid,[12,13] and sudden changes in the orientation of

a)Electronic mail: hartkamp@mit.edu
b)Electronic mail: benoit.coasne@enscm.fr

water molecules.[14–18] Transport coefficients are also important to describe the dynamics of aqueous electrolytes.[19–21] Reconciling knowledge about hydration structure with the shear viscosity and self-diffusion is of paramount importance for the improvement of applications in tribology, mixing, separation, desalination, osmosis, and lab-on-a-chip devices.[22–24]

The majority of computational studies of the structure and dynamics of aqueous electrolytes is focused on a subset of the halogen group (anions) and the alkali metals (cations). In particular, sodium (Na^+), potassium (K^+), calcium (Ca^{2+}), and chloride (Cl^-) form a vital component in almost all biological systems, including the human body and seawater. In contrast, radioactive ions, such as cesium (Cs^+) and strontium (Sr^{2+}), have received much less attention. Nature is sometimes exposed to harmful isotopes of cesium and strontium as a consequence of nuclear testing, nuclear weapons or accidents, such as the Fukushima disaster in 2011. Such exposure is especially dangerous due to the fact that living organisms tend to mistake cesium for potassium and strontium for calcium.[25–28] This can directly or indirectly lead to ingestion by humans or animals, which is very dangerous due to highly ionizing radiation. Similarly, the resemblance between strontium and calcium makes that strontium can easily end up in bones or fluid electrolyte systems of living organisms. Preventing this by selectively removing these ions from bulk salt water is very difficult and requires more understanding of the hydration structure and dynamics of ion hydration and ion-ion pairing. This is especially true for strontium, which has been included in very few computational studies.[29,30] Understanding the pairing and solvation properties of these ions hopefully contributes to finding a process to discriminate between them.[31–33]

One of the purposes of this work is to compare hydration properties and ion pairing of conventional and radioactive ions with each other. We attempt to do this by discussing and unifying results for various structural and dynamic quantities of five different cations and three ion concentrations. In addition to some of the more common measures of hydration structure (radial distribution function, coordination number, and orientation of water molecules), we also study the hydrogen bonding around ions in a way that provides more microscopic insight by showing information that is often lost due to spatial averaging. These hydrogen bonding profiles can elucidate the effect of ions on the hydrogen bond network of water. Computer simulations are extremely suitable to study this. However, in most computational studies of spatially homogeneous fluid, the data are averaged over the domain in order to enhance the statistics at the cost of microscopic detail. Our novel approach shows the differences in hydrogen bonding in the first hydration shell around various cations. These differences in the hydrogen bond network are paramount to understanding the dynamics of electrolyte solutions. The dynamics of the solution is discussed in terms of the self-diffusion and shear viscosity, while the dynamics of hydration and ion pairing are studied in terms of a pairing time scale that avoids the usual assumption of an exponentially decaying correlation function and has physical significance regardless of the problem at hand.

It is expected that the structure and dynamics of Ca^{2+} and Sr^{2+} are very similar since both ions are small and bivalent, thus allowing for strong electrostatic binding with other ions and water molecules. On the other hand, K^+ and Cs^+ are both characterized by a single valence and a large diameter, which is also expected to result in similarities between the properties of these ions. Our intention is to identify small differences between ions that could be enhanced, for example, in a porous material.[34,35] Examples of such possible differences are: ion pairing, hydrogen bonding, and diffusion.

The remaining part of this paper is organized in four sections. In Sec. II we discuss the molecular simulations. Various structural properties are studied in Sec. III. We then study the dynamics in Sec. IV. Finally, Sec. V summarizes our findings and conclusions.

II. MOLECULAR SIMULATIONS

The salt concentrations in seawater and in most living organisms are of the order of $10^{-3} - 10^{0}$ M. Many computational studies of electrolyte solutions focused on the structure and dynamics of ions in water in the dilute limit, which is ideal for the study of ion-solvent interaction.[36] Many other studies focused on brine salt solutions (i.e., solutions with a very high ion concentration, 1–4 M), in which ion-ion interactions can be studied with relatively low computational cost.[37,38]

In this work, 15 aqueous electrolyte solutions are simulated. The anion in each simulation system is Cl^- while five different cations are considered: Na^+, K^+, Cs^+, Ca^{2+}, and Sr^{2+}. Salt concentrations of approximately 0.3 M, 0.6 M, and 0.9 M are considered. The number of monovalent anions and cations are equal, while the number of bivalent cations at the same salt concentration is half that of the anions to ensure electroneutrality of the system.

A. Models and force fields

The water molecules are represented by the TIP4P/2005 rigid water model of Abascal and Vega.[39] This water model has shown to be reasonably successful in reproducing the structure and transport coefficients of water.[40–42] However, this model has not yet been tested much for simulating aqueous solutions. Therefore, we use ion force field parameters from the literature that have been optimized in combination with other rigid water models.[43–46] The force field parameters that we use have been optimized for SPC/E water (except those for Na^+ and Cl^- which have been optimized for the RPOL water model but are very close to parameters that have been optimized for SPC/E).[44] The interactions are described by the combination of a Lennard-Jones potential and Coulombic interactions. The Lennard-Jones parameters and charges are listed in Table S I in the supplementary material.[47] The Lorentz-Berthelot mixing rules are used to calculate cross-species interaction parameters from the parameters listed in the table. The transferability of various pairwise additive ion force field parameters have been tested between different non-polarizable water models[48–50] as well as between

non-polarizable and polarizable models.[51–53] Good transferability has been confirmed for various monovalent force field parameters close to those used here. For the bivalent ions, we use parameters that have recently been presented by Mamatkulov *et al.*[46] These parameters have been optimized to match the experimental solvation free energy and activity coefficient for pairing with various halides. In order to validate that the ion force fields parameters are suitable to use in combination with TIP4P/2005 water, we compare the hydration structure of the five different cations in 0.3M aqueous chloride solutions with TIP4P/2005 water and with SPC/E or RPOL polarizable water. These results are shown in Figure S1 in the supplementary material.[47] The figure also shows the radial distribution functions of sodium and chloride ions are compared to those calculated by Smith and Dang[54] for SPC/E and (polarizable) RPOL water. Good agreement is found between our results for the different water models as well as with the comparison to the results from Smith and Dang.[54] Our structural data for the solutions with TIP4P/2005 will be discussed further in Sec. III. While non-polarizable force fields have been widely applied and accepted for the past few decades, these force fields have been known to sometimes lead to excessive ion-pair formation. Explicitly including polarizability in the force field can become especially relevant near a liquid/vapor interface, where the symmetry of the hydration shell is broken.[55] While polarizable force fields can increase the accuracy in these situations, the large computational cost of these calculations introduces a limitation on the feasible size of the simulation system.

B. Simulation details

Systems are prepared by first estimating the number of water molecules in a cubic periodic box of 50 × 50 × 50 Å, where the water has a temperature of 300 K and a pressure of 1 atm. Based on this estimate, the required number of ions is inserted in the box to produce the correct ion concentration. Next, grand canonical Monte Carlo (GCMC) simulations are run to add, remove, translate, and rotate water molecules until a thermodynamic equilibrium is reached with the chemical potential corresponding to the bulk saturation vapor pressure of the water model.[40] NPT simulation, in which the number of water molecules is fixed and the system volume is adjusted until the correct pressure is reached, would also have been possible. Figs. S2 and S3 in the supplementary material[47] show that our GCMC simulations allow reproducing available literature data on the effect of concentration on the density and energy of aqueous electrolytes. The resulting configuration is used as the input for classical Molecular Dynamics (MD) simulations. We show the packing fractions of the solution in Table S II in the supplementary material.[47] Despite the presence of van der Waals forces and Coulombic interactions the packing fractions of the solutions are very similar to those typically observed in granular materials[56,57] and dense hard sphere fluids.[58] Figures S2 and S3 in the supplementary material[47] show the mass density and total energy of the simulation systems. The mass density in Figure S2 of the supplementary material[47] is shows to agree very well with experimental data.

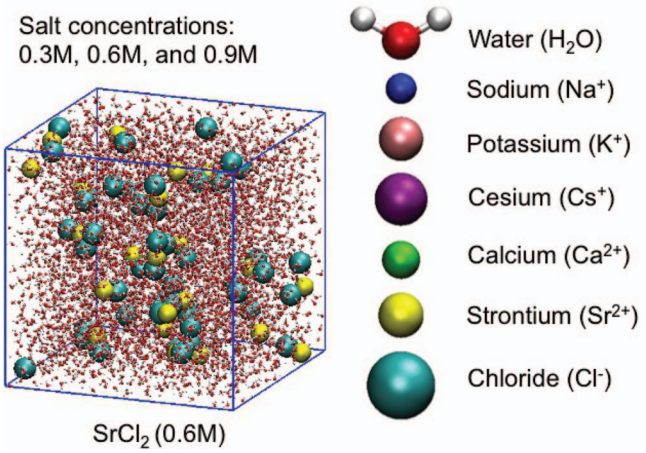

FIG. 1. A typical molecular configuration of an aqueous $SrCl_2$ solution. The salt concentration is 0.6M. The simulation box has a size $L = 50$ Å and is periodic in each direction. The water molecules are displayed small for the sake of visibility. The top and right of the figure shows an overview of the species and concentrations that are considered in this study.

The greatest discrepancy is seen for the NaCl solution, for which the density of the simulated solution is overestimated by approximately 1.5%. A comparable overestimation of the density has been found for a NaCl solution with the ion force field optimized by Joung and Cheatham[59] in combination with the SPC/E water model.[60] The SHAKE algorithm is used to preserve the rigid structure of the water molecule. The dispersion interactions in the fluid are described by a Lennard-Jones potential, with a cutoff length of 12 Å. The Particle-Particle-Particle-Mesh (P^3M)[61] method is used to calculate electrostatic interactions, where we truncate the real part at 12 Å. Figure 1 shows a snapshot of the system containing a $SrCl_2$ solution with a concentration of 0.6M. The MD simulations are performed in the canonical ensemble, where the temperature is controlled using a Nosé-Hoover thermostat.[62] The equations of motion are integrated using the velocity Verlet scheme with a time step of 1 fs. After an equilibration period, data are accumulated from a 5 ns steady-state simulation.

III. STRUCTURE

A. Structure in aqueous electrolyte solutions

Figure 2 shows the cation-anion (a) and cation-oxygen (b) radial distribution functions (RDF). These RDFs correspond to a salt concentration of 0.3M, while those corresponding to concentrations of 0.6M and 0.9M are omitted for the sake of visibility. The dependence of the RDFs on the salt concentration is discussed in the text below. The RDF denotes the density of an atom species (relative to its bulk density) as a function of the distance from a given atom. These radial density functions can also be used to calculate coordination numbers N_C, i.e., the number of neighboring atoms within a certain distance r_{max}:

$$N_C = \frac{4\pi N}{V} \int_0^{r_{max}} g(r) r^2 \, dr, \tag{1}$$

where N is the number of atoms and V is the volume of the simulation box. The value for r_{max} is typically chosen to be the

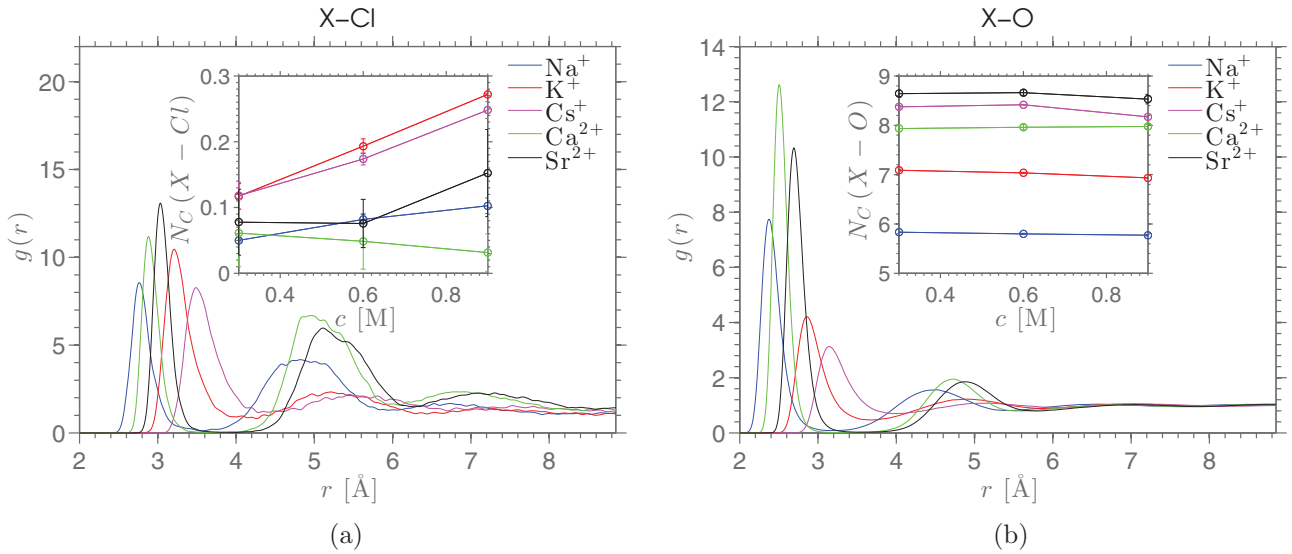

FIG. 2. Radial distribution functions $g(r)$ of (a) cation-anion (X-Cl) pairs and (b) cation oxygen (X-O) pairs. The profiles correspond to a salt concentration of 0.3M. The profiles corresponding to concentrations of 0.6M and 0.9M are omitted for the sake of visibility. The different colors of the lines correspond to the cations species in the chloride solutions: Na^+ (blue), K^+ (red), Cs^+ (magenta), Ca^{2+} (green), and Sr^{2+} (black). The insets in the figures show the coordination numbers N_C of the first hydration shell along with the standard error denoted by the error bars. The error bars in the inset of (b) are smaller than the symbols.

radius of the first hydration shell, defined by the position of the first local minimum in the RDF. The coordination numbers for the first hydration shell are shown in the insets of Figure 2. The error bars in the insets denote the standard error of the coordination numbers. The number of water molecules in the first shell around an ion is also called the hydration number. We will show in this section that the hydration number can be large when the ion is large (resulting in a large hydration shell) or when the binding strength between an ion and water is large (resulting in a dense hydration shell).

The locations of the extrema in the RDF do not depend on the ion concentration. On the other hand, the magnitude of the peaks in the cation-anion distribution decreases with increasing molarity. This is easily understood since the RDF denotes a density normalized by the bulk density (i.e., by the salt concentration in the case of a cation-anion RDF). We first discuss the cation-anion RDF and corresponding coordination numbers and later those for cation-oxygen ("oxygen" refers of the oxygen atom in a water molecule). The inset in Figure 2(a) shows that the average number $N_C(X - Cl)$ of anions Cl^- in the first shell of cations X (where $X = Na^+, K^+, Cs^+, Ca^{2+}, Sr^{2+}$) increases with the ion concentration. The increase in $N_C(X - Cl)$ with the ion concentration is the largest for K^+ and Cs^+. Considering that K^+, Cs^+, and Cl^- are large ions, this result is consistent with the known association behavior of ions dissolved in water; small ions do not associate with large ions, while large ions do associate with other large ions of opposite charge.[1,63] The ion-ion coordination number of monovalent electrolytes is a direct measure of the portion of electrolytes that is associated. This is only approximately true for bivalent ions because these electrolytes can partially dissociate by loosing one chloride ion. The coordination numbers in the inset of Figure 2(a) show that a dissociated state is favorable for $CaCl_2$ and $SrCl_2$ in water; two anions are available per cation, yet the coordination numbers $N_C(X - Cl)$ barely reach 0.1 at these low molarities. This can be explained by the fact that the bivalent cations have a stronger interaction with nearby water molecules than with monovalent anions. In other words, dehydration of the bivalent cation would cost more energy than what is gained by forming a pair with a chloride ion.[64] The ion-ion coordination numbers could even turn out a bit lower if a polarizable water model would be used. Indeed, an overestimation of the cation-anion association is known to arise when a non-polarizable water model is used,[65] while other structural properties are not strongly dependent on the polarizability of the water molecules.[55] The negative effect of polarizability on ion pairing is expected to have the strongest influence on the bivalent ions due to their large charge density.

The cation-oxygen RDFs (Figure 2(b)) for different ion concentrations overlap almost perfectly (only concentration 0.3M is shown here for visibility), while the coordination numbers in the inset of Figure 2(b) show a hint of a decrease with increasing ion concentration. This is not surprising, since a larger portion of the hydration shell is occupied by ions when the ion concentration is large (hence the increase of $N_C(X - Cl)$ with increasing ion concentration). An overview of the coordination numbers $N_C(X - O)$ calculated in this study to those reported in the literature is given in Table S III in the supplementary material.[47] As expected, the coordination numbers and the hydration shell radius r_{max} of the monovalent ions increase with their Lennard-Jones size parameter σ. Dividing N_C by the surface area of the bare Lennard-Jones sphere ($A = \pi\sigma^2$) gives an estimate of the extend to which the ions are chaotropic or kosmotropic.[43] Table I shows for the different cations the coordination number and the number of water molecules (oxygen atoms) per square Angstrom of surface area $\tilde{N}_C = N_C/A$. The data corresponds to a concentration of 0.3M. A large $\tilde{N}_C$ indicates that the ion is a kosmotrope. We find that calcium is more kosmotropic than strontium, which could be an advantage for the selective removal of strontium from water. According to this

TABLE I. Cation-oxygen coordination number N_C and coordination number divided by the surface area of the cation $\tilde{N}_C = N_C/A$. These data correspond to chloride solutions with a concentration of 0.3M. The fourth column shows the Lennard-Jones diameters σ (expressed in Å) of the cations. The last column shows the outer radius of the first hydration shell r_{max} (expressed in Å).

	N_C	$\tilde{N}_C$	σ	r_{max}
Na^+	5.80	0.34	2.3359	3.18
K^+	7.09	0.2	3.332	3.68
Cs^+	8.38	0.18	3.884	3.99
Ca^{2+}	7.88	0.43	2.41	3.34
Sr^{2+}	8.59	0.28	3.1	3.6

quantity, strontium is less kosmotropic than sodium, despite its larger valence. The Na^+ RDFs show very similar behavior as those of the bivalent ions; strong electrostatic interactions with neighboring atoms and ions are possible due to the small size of Na^+, whereas in the case of the bivalent ions the electrostatic interactions are strong due to their larger charge. These three ions have a large charge density and are considered kosmotropic, whereas K^+ and Cs^+ have a lower charge density and are said to be chaotropic. The pronounced peaks in the RDFs of the former group of ions are separated by a region where virtually no anions or oxygen atoms are found. This border between the first and second hydration shell is characterized by an energy barrier that can be read from the difference between a local maximum and minimum in the potential of mean force: $U_{PMF}(r) = -k_B T \ln(g(r)) + C$ where C is a constant. The larger the barrier, the more energy is required for a particle to leave the hydration shell. Note that a theoretical local minimum value of zero in RDF would correspond to an infinite energy barrier prohibiting particles from entering or leaving the first hydration shell. The pairing dynamics in Sec. IV will demonstrate that atoms do in fact cross the barriers.

The data in Figure 2 provide insight in the radial structure around ions. However, the orientation of water molecules and the distribution of hydrogen bonds are also important for a thorough analysis of structural properties in aqueous electrolyte solutions. Hydrogen bonds[66–69] are held responsible for the fact that water is a highly structured liquid.[7] Yet, microscopic understanding of hydrogen bonding in water is limited, despite active research.[14,67,70–72] The influence of ions on the surrounding hydrogen bonds has been studied predominantly in the context of average bonding times and hydration shell-averaged number of hydrogen bonds.[7,73,74] In Sec. III B, we present an alternative approach to study the structure of the hydrogen bond network around a hydrated ion.

Hydrogen bonds can be defined based on geometry,[75,76] topology,[77,78] energy criteria,[79] or combinations of these.[80] The average number of hydrogen bonds in bulk water at room temperature and atmospheric pressure varies between 2.8 and 3.5, depending on the hydrogen bond definition and on the water model.[81] We follow here a geometrical definition based on a combination of the $O\cdots H$ distance $r_{OH} < 2.35$ Å and the $O_j - O_i\cdots H_i$ angle $\angle_{OOH} < 30^\circ$, where molecule i is the donor molecule and j the receiver.[76] The distance and angle

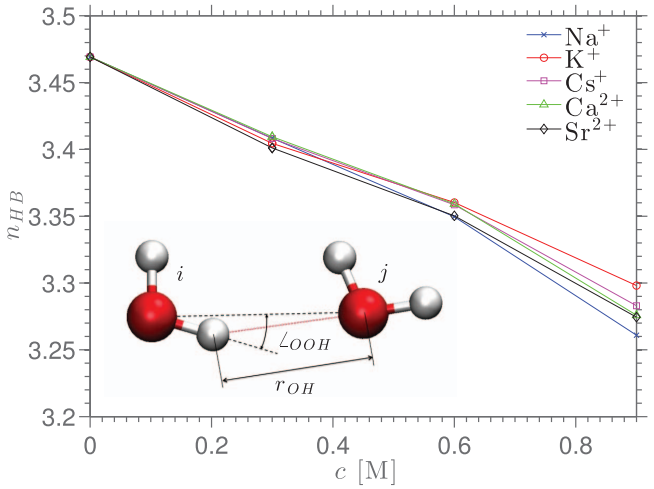

FIG. 3. Average number of hydrogen bonds per water molecule for different aqueous chloride solutions and different electrolyte concentrations at a temperature of 300 K and a pressure of 1 atm. The different colors of the lines correspond to the cations species in the chloride solutions: Na^+ (blue), K^+ (red), Cs^+ (magenta), Ca^{2+} (green), and Sr^{2+} (black).

relevant for the bonding criterion are shown in the inset of Figure 3. Figure 3 shows the average number of hydrogen bonds (n_{HB}) per water molecule as a function of the ion concentration for the different aqueous electrolytes considered in this work. The number of hydrogen bonds decreases almost linearly with increasing ion concentration. The slope is the smallest in the presence of the chaotropic cations K^+ and Cs^+. The decrease in n_{HB} is expected to continue at much larger ion concentrations, where ion-specific effects become more pronounced.[82,83] However, this would still provide little information about the extent and way in which a single ion disturbs the water structure in its direct environment.

Another approach to study ion-specific effects on hydrogen bonding is to measure n_{HB} in the hydration shells around the ions,[84,85] as will be done below.

B. Ion-solvent structure

We have performed a series of MD simulations at infinite dilution in order to study the structure around solvated ions without having interference from ion-ion interactions. Furthermore, the influence of Lennard-Jones parameters and the ion valence are studied. These data are discussed in the remaining part of this section about structural properties. The simulations were prepared and performed in a similar fashion as what was explained in Sec. II, but instead of having various ion pairs, a single anion and cation are fixed at a distance of 25 Å, in a simulation cell of 50 × 25 × 25 Å in size. The charge of the anion is chosen to compensate the cation charge, such that the system remains neutral. Only the cation-solvent structure is discussed here.

Figure 3 showed that the number of hydrogen bonds per water molecule in an aqueous solution deviates from that in pure water. This indicates that ions disturb the hydrogen-bond network of water molecules located in their hydration shell ($\tilde{n}_{HB}$). Hydration shell-averaged values of $\tilde{n}_{HB}$ have been shown to increase with the size of the cation.[84,85] However,

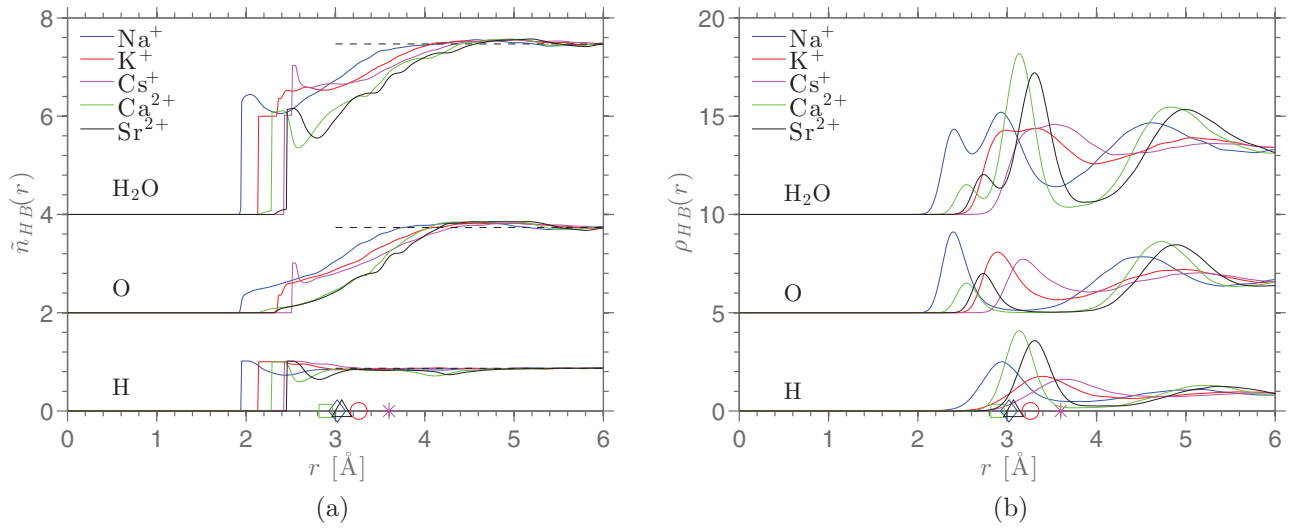

FIG. 4. Number of hydrogen bonds per water molecule ($\tilde{n}_{HB}$) as a function of the distance to a solvated cation (a) and the density of hydrogen bonds in the hydration shells around various cations at infinite dilution (b). These profiles (top) are decomposed into the contribution of the donor (bottom) and receiver (middle). The markers on the horizontal axis denote the radius of the first hydration shell and the profiles on top (H_2O) and in the middle (O) are vertically shifted up (by 4 and 2, respectively) for visibility. The different colors of the lines correspond to the cations species in the chloride solutions: Na^+ (blue), K^+ (red), Cs^+ (magenta), Ca^{2+} (green), and Sr^{2+} (black). The black dashed lines correspond to the number of hydrogen bonds in pure bulk water.

microscopic details are lost in the averaging over the hydration shell. In order to preserve this information, we show in Figure 4(a) the number of hydrogen bonds per water molecule as a function of the distance from the center of the cation. This function is decomposed in the number of hydrogen bonds per hydrogen atom (bottom) and per oxygen atom (middle). The markers on the horizontal axis denote the radius of the first hydration shell and the profiles on top and in the middle are vertically shifted up for visibility. The profiles for water show that $\tilde{n}_{HB}$ drops below its bulk value in the first hydration shell. On the other hand, each profile shows a maximum in the second hydration shell that slightly exceeds their bulk values. This is consistent with the findings of Guardia *et al.*,[85] who reported values for $\tilde{n}_{HB}$ averaged over the first and the second hydration shells around monovalent ions.

The hydrogen profiles (bottom) reach a plateau on the left corresponding to exactly one hydrogen bond per hydrogen atom. This value is larger than in bulk water (where we find $3.47/4 = 0.87$ hydrogen bonds per hydrogen atom). The bulk and the plateau on the left are separated by a small trough in the case of kosmotropic cations, whereas the chaotropic cations show a smooth transition from the plateau to the bulk value. The same trough arises again in the second hydration shell. The first trough occurs on the outside of the first shell while the second one is located on the inside of the second shell. These troughs indicate that these positions, in combination with the preferred orientation of the water molecules, are not optimal for hydrogen atoms to form a hydrogen bond with neighboring water molecules. This is discussed in more detail later in this section.

Each of the oxygen profiles (middle) shows a significant decrease in the first hydration shell with respect to the bulk value. A clear difference is seen between the monovalent and bivalent ions; the oxygen atoms in the first hydration shell around a monovalent cation receive hydrogen bonds, which is not the case for the oxygen atoms in the dense hydration shell around the bivalent ions. A highly structured cage of water molecules around the bivalent cations was implied by the thin and high peaks in Figure 2(b). The result in Figure 4(a) reveals that this cage is not kept together by hydrogen bonds, which implies that the electrostatic interactions between the ion and the water molecules are alone responsible for the first hydration shell around the bivalent ions. On the other hand, electrostatics and the hydrogen bonds both play an important role in the first hydration shell around the monovalent ions. Hence, the hydrogen bond network around Na^+ deviates from that around the bivalent ions, while the other structural properties showed a close similarity between Na^+ and the bivalent cations.

Multiplying the profiles shown in Figure 4(a) with their corresponding RDFs results in the radial density of hydrogen bonds shown in Figure 4(b). Most of the ions show a large density of receivers in the first hydration shell, which is balanced by a large density of donors in the second shell. However, the Na^+-profiles deviate from this picture and show a large density of both receivers and donors in the first hydration shell. This result indicates that many of the water molecules close to Na^+ form hydrogen bonds with other molecules in the same shell. Water molecules in the first shell around other cations form hydrogen bonds primarily with water molecules in the second shell.

In order to further study the effect of ion valence, the hydration structure of Sr^{2+} was compared with that of a monovalent ion having the same Lennard-Jones parameters (Table S I in the supplementary material).[47] Figure 5 shows the radial structure around Sr^{2+} (top), as well as around its monovalent equivalent (bottom). The figure shows the cation-oxygen (g_{XO}) distribution in black, cation-hydrogen (g_{XH}) in red, and $\tilde{n}_{HB}$ in green. The dashed lines indicate bulk values while the blue and magenta lines are the decomposition of $\tilde{n}_{HB}$ into the number of hydrogen bonds per oxygen (receiver) and per hydrogen (donor) atom. The magnitudes of

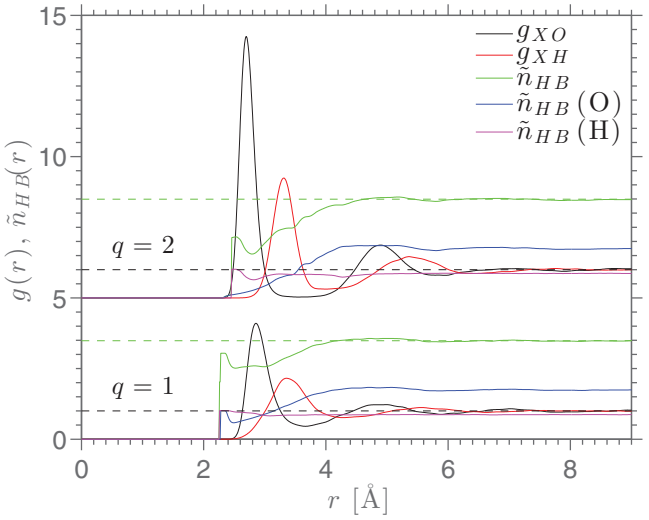

FIG. 5. Radial distribution function and hydrogen bonding distribution of Sr^{2+} ($q = 2$) and a monovalent ion ($q = 1$) with identical Lennard-Jones parameters ($\sigma = 3.1$ Å and $\epsilon = 0.25$ kcal/mol). The strontium curves ($q = 2$) are shifted 5 up for visibility. The figure shows the cation-oxygen (g_{XO}) interaction in black, cation-hydrogen (g_{XH}) in red, and the number of hydrogen bonds per oxygen atom ($\tilde{n}_{HB}$) in blue. The dashed lines indicate bulk values. The blue and magenta lines are the decomposition of $\tilde{n}_{HB}$ into the number of bonds per oxygen (receiver) atoms and per hydrogen (donor) atom.

the peaks in g_{XO} and g_{XH} are smaller for the monovalent ion. Moreover, the positions of the extrema are further away from the ion and the energy barriers between the hydration shells are lower (seen from calculating the potential of mean force, as explained previously). A lower energy barrier would correspond to a shorter average residence time (this will be discussed in Sec. IV). Overall, the monovalent ions are less kosmotropic than their bivalent equivalent. Figure 5 also confirms that a smaller charge allows for more hydrogen bonds per oxygen and hydrogen atom close to the ion. The strong electrostatic interactions around a bivalent ion result in a very dense hydration shell with a smaller radius than those around monovalent ions of the same size. The large density of the shell and the strong electrostatic interactions reduce the rotational freedom of the water molecules, such that they cannot orient themselves to favor the formation of hydrogen bonds. Furthermore, the RDFs indicate that the inner part of the hydration shell is depleted of hydrogen atoms to bond with. This implies a highly preferred orientation of the water molecules with respect to the cation. Finally, the larger curvature of the smaller hydration shell could make it increasingly difficult for neighboring water molecules to adopt an orientation relative to each other that allows for the formation of a hydrogen bond. Confirming this argument would require further investigation. Instead, we focus in what follows on the suggested relation between hydrogen bonding and the orientation of water molecules relative to a hydrated cation.

Lee and Rasaiah[86] showed that the smearing of the orientation distribution of water molecules around monovalent cations increases with their Lennard-Jones diameter. Here we will confirm this observation and also look at the influence of the ion charge and the Lennard-Jones energy parameter. Two angles are used to describe the orientation of a water molecule with respect to a cation.[87–89] The first angle θ is defined as the smallest angle between the dipole vector of the water molecule and the axis intersecting the cation and the oxygen atom. The other angle ϕ is spanned by the cation-oxygen interaction vector and the vector from the oxygen to the hydrogen atom that makes the smallest angle with the cation-oxygen vector. Figure 6 shows the probability distributions of the angles θ and ϕ that describe the orientation of water molecules in the first hydration shell around a cation. The distributions that correspond to the monovalent ions are consistent with those reported by Lee and Rasaiah.[86] Furthermore, the narrow angle distributions of the bivalent ions confirm the expected enhanced structural ordering. The dashed black lines correspond to the monovalent ion with the Lennard-Jones parameters of strontium. The angle probability distributions of this ion overlap with those of K^+, as do their RDFs (see

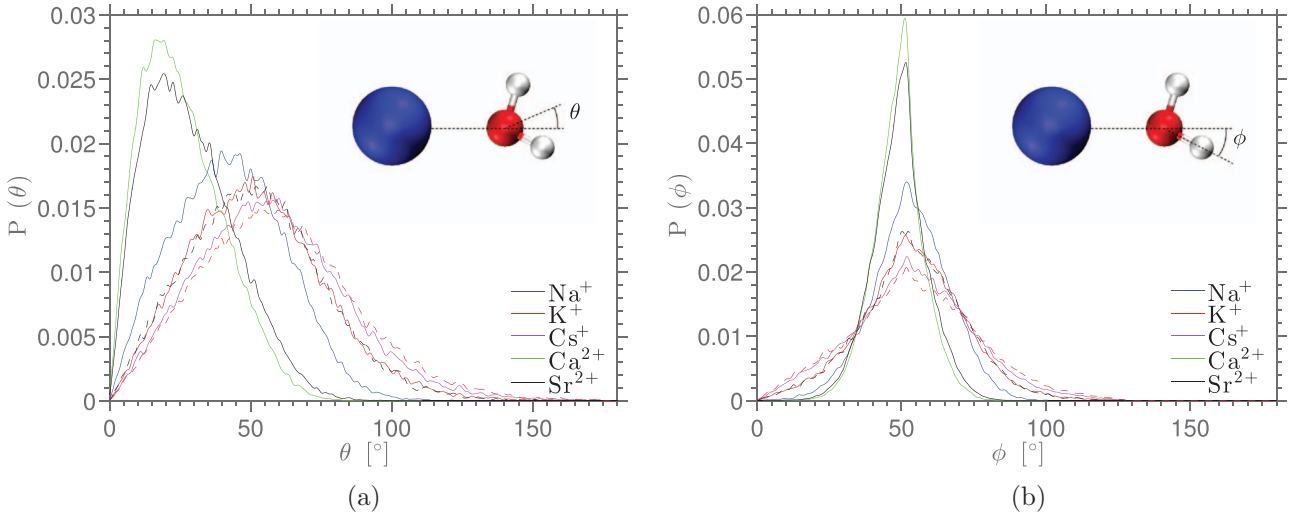

FIG. 6. Probability distribution of the orientation angles θ (a) and ϕ (b) of water molecules in the first hydration shell around a cation at infinite dilution. The definitions of the angles are shown in the right upper corner of the figures. The different colors of the lines correspond to the cations species in the chloride solutions: Na^+ (blue), K^+ (red), Cs^+ (magenta), Ca^{2+} (green), and Sr^{2+} (black). The red dashed lines correspond to potassium with a stronger Lennard-Jones energy parameter $\epsilon = 1$, while the dashed black lines correspond to a monovalent ion with its Lennard-Jones parameters equal to those of strontium.

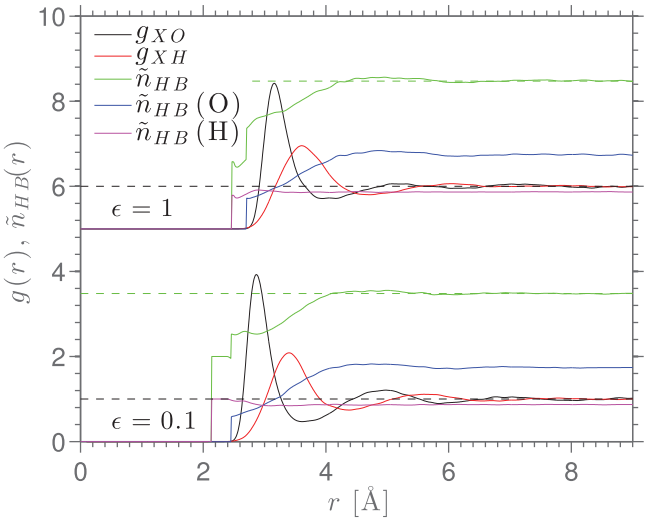

FIG. 7. RDF and hydrogen bonding distribution of K^+ ($\epsilon = 0.1$ kcal/mol) and an ion with a much larger Lennard-Jones energy parameter $\epsilon = 1.0$ kcal/mol (but the same size and valency). The curves corresponding to the latter ion ($\epsilon = 1.0$) are shifted 5 up for visibility. The figure shows the cation-oxygen (g_{XO}) interaction in black, cation-hydrogen (g_{XH}) in red, and $\tilde{n}_{HB}$ in green. The blue and magenta lines are the decomposition of $\tilde{n}_{HB}$ into the number of bonds per oxygen (receiver) atoms and the number per hydrogen (donor) atom, respectively. The green dashed lines indicate the number of hydrogen bonds per water molecules in pure bulk water, and the black dashed lines indicate the bulk limit of the RDF, $g(r) = 1$.

Figures 2(b) and 5). This similarity in structure between ions with different Lennard-Jones parameters implies that the difference between the Lennard-Jones diameters might be counterbalanced by a difference in the energy parameters. In order to study the influence of the energy parameter, an ion is introduced with the same charge and diameter as potassium but with a Lennard-Jones energy parameter that is ten times larger: $\epsilon = 1.0$. The data corresponding to this ion is represented by the red dashed lines in Figure 6 and the radial structure is shown in Figure 7. The effect of the Lennard-Jones energy parameter on the hydration structure is indeed very similar to the effect of the diameter. We find that a small ion with a large interaction strength ϵ can have a similar solvation structure as a large ion with a small interaction strength, despite the obvious difference between the Lennard-Jones potentials of both ions. The radius of the hydration shell and the charge density of ions thus depends on all three parameters discussed here: σ, ϵ, and q.

The angle distributions have also been calculated from the simulations data with 0.3M ion concentration. Averaging the data over all cations present in the system results in a more smeared distribution since nearby ions disturb the structure of the hydration shells. When we exclude the ions that are within 10 Å of another ion, we obtain the same ion-solvent angle distribution as in the case of infinite dilution.

IV. DYNAMICS

It was already mentioned in Sec. III that the RDF can be used to gain insight in the energy needed to enter or leave a hydration shell. This information, in the framework of the transition state theory, can be used to estimate the corresponding characteristic time. Notwithstanding the convenience of such an approach, it does not alleviate the need for directly studying the dynamics of the system.

A. Self-diffusion

The self-diffusion coefficient D of ions and water in aqueous solutions can be calculated using the Green-Kubo formalism, which requires the evaluation of the atomic velocity-autocorrelation function. This expression can equivalently be written in terms of a mean squared displacement, called the Einstein relation.[90] We evaluated the Einstein relation for the ions and water to calculate the diffusion coefficients of the different species present in the fluid. Figure 8 shows the self-diffusion coefficients D as a function of the ion concentration. The full lines are for the cations, the dashed lines are for the anions, and the dashed-dotted lines are for the oxygen atoms of water. The self-diffusion coefficient for pure TIP4P/2005 water ($D = 2.35 \times 10^{-9}$ m^2/s), which was measured in a simulation box of 50 Å, is consistent with the value predicted by Tazi *et al.*[19] The self-diffusion coefficient of water decreases when ions are added to the solution and continues to decrease with an increasing salt concentration. The strongest decrease is seen for Na^+, Ca^{2+}, and Sr^{2+}, while a smaller decrease is seen for electrolyte solutions that contain K^+ or Cs^+. The fact that the water becomes less diffuse with increasing ion concentration indicates that the electrolytes reduce the mobility of the water molecules, for example, by forming hydration shells; when ions diffuse together with their surrounding water cage it reduces the overall mobility of the water. If the ions indeed enhance the fluid structure, then the velocity-autocorrelation functions of the ions are expected to show oscillations rather than a monotonic decay to zero. This is

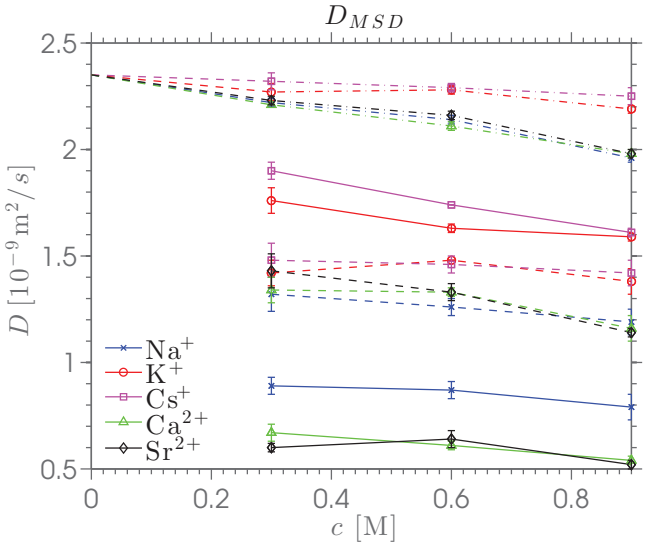

FIG. 8. Self-diffusion coefficients D as a function of the electrolyte concentration: (full lines) cations, (dashed lines) chloride, and (dashed-dotted lines) oxygen atoms of water for all electrolyte solutions. The different colors of the lines correspond to the cations species in the chloride solutions: Na^+ (blue), K^+ (red), Cs^+ (magenta), Ca^{2+} (green), and Sr^{2+} (black). The diffusion coefficients are calculated from the mean squared displacement (MSD). The standard error is denoted by the error bars.

confirmed by Figure S4 in the supplementary material,[47] showing oscillatory structures in the velocity-autocorrelation functions for Na^+, Ca^{2+}, and Sr^{2+}. A slower and more monotonic decay to zero is observed for K^+ and Cs^+. The slower decay of the correlation function of Cs^+ could be due to the fact that this ion is much heavier than K^+. The self-diffusion of the ions also shows a difference between the behavior of Na^+, Ca^{2+}, and Sr^{2+} on the one hand, and K^+ and Cs^+ on the other. The self-diffusion coefficients of K^+ and Cs^+ are close to those of water while Na^+, Ca^{2+}, and Sr^{2+} show much slower diffusion. This observation is consistent with the result for monovalent ions presented in Ref. 88. This result indicates that the kosmotropic ions (plus their hydration shells) have a larger effective friction than the chaotropic ions, which do not hold on as tightly to their hydration shells. The ion diffusion coefficients are lower than experimentally measured diffusion coefficients reported in the literature.[4,91–93] This was also observed by Walter *et al.*,[94] who compared the diffusion of Na^+ and Cl^- in three different water models. The diffusion coefficient of pure TIP4P/2005 was closer to the experimental value than those calculated for SPC/E and TIP4P water. However, when ions were present, the diffusion coefficients of the ions in TIP4P/2005 were smaller than those measured in experiments and in simulations with SPC/E or TIP4P. Ion force field parameters optimized to be used in combination with TIP4P/2005 could perhaps be more successful in closely reproducing experimental diffusion coefficients.

The fact the diffusion coefficient of the water molecules decreases with an increasing ion concentration (we will refer to this behavior as structure making) for each of the solutions is a known discrepancy between simulations and experimental measurements. Indeed experimental data suggests that the opposite trend (corresponding to structure breaking behavior) is also observed. Kim *et al.*[21] compared different water models and simulation parameters, and found no structure breaking behavior. They remarked that molecular models are commonly developed by choosing a functional form and optimizing the parameters. Such an approach does not guarantee that the functional form of the resulting model is suitable to reproduce the transport properties of electrolyte solutions. Also polarizable force fields have not shown to be successful in reproducing the correct qualitative trends in the diffusion coefficient of electrolyte solution.[53] The problem of anomalous self-diffusion coefficients of aqueous solutions in MD simulations has been revisited recently by Ding *et al.*[95] They compared results of classical MD and *ab initio* molecular dynamics (AIMD) simulations for CsI and NaCl solutions with a salt concentration of 3M. The AIMD simulations were able to qualitatively reproduce the structure breaking behavior for a CsI solution (i.e., an increasing diffusion coefficient with increasing salt concentration) observed in experiments. No striking differences were observed between the radial distribution functions calculated from AIMD and classical MD. The authors found a dynamic heterogeneity in the AIMD simulations which is not present in the classical MD simulations. As a result, it was suggested that this feature is crucial to reproduce structure breaking behavior. These recent findings illustrate that the ability of simple classical models to correctly reproduce experimental diffusion coefficients requires further study. Dynamics is often overlooked in the development of force fields. The functional form of current classical potentials are often chosen *a priori* , while the corresponding parameters are optimized to reproduce structural or thermodynamic quantities.

B. Ion-ion and ion-water pairing dynamics

The ion-ion and ion-water pairing dynamics can be studied via the widely applied definition introduced by Impey, Madden, and McDonald.[8] These authors defined a residence function $\chi(t)$ as the time correlation of a binary switch $P_{ij}(t)$ that indicates if ions i and j are a pair at time t:

$$\chi(t) = \sum_{i=1}^{N_X} \sum_{i=j}^{N_Y} \langle P_{ij}(0) P_{ij}(t) \rangle, \tag{2}$$

where N_X is the number of cations and N_Y is the number of anions or water molecules, depending on which pairing function is calculated. The angular brackets in Eq. (2) denote that the correlation function is averaged over multiple trajectories.[96] Ions i and j are considered "paired" if the distance between them is in the first shell of the corresponding RDF (Figure 2). A tolerance time of 2 ps is implemented to allow for a temporary separation directly followed by a return to the first shell. We define a normalized residence function $\tilde{\chi}(t) = \chi(t)/\chi(0)$ by dividing $\chi(t)$ by the number of pairs at its origin $\chi(t = 0)$ such that $\tilde{\chi}(0) = 1$. Hence, $\tilde{\chi}(t)$ can be interpreted as the probability that a pair exists at a time t, knowing it exists at a time $t = 0$. The MRT of an ion-ion or ion-water pair can be non-uniquely calculated from $\tilde{\chi}(t)$. The most commonly used definition for the MRT is the time integral over the residence function.[8,20,97] This definition of the MRT is based on the assumption that the residence function decays exponentially, in which case the time integral equals the decay rate of the exponent. However, the assumption of exponentially decaying correlations tends to be inaccurate at short times for dense liquids,[98] such that the integral over the residence function loses its physical interpretation of being the decay rate of the exponential.

Here, we propose an alternative definition, which is easy to calculate and physically meaningful regardless of the functional form of the residence function. We define the residence time τ in terms of the first moment of a probability distribution function that can be derived from $\chi(t)$. If we consider an initial (ensemble averaged) set of ion-ion or ion-water pairs given by $\chi(0)$, the rate of dissociation of these pairs is $B(t) = d\chi(t)/dt$. Since the total number of pairs in an equilibrium bulk fluid is constant in time (apart from statistical fluctuations) the function of association and dissociation have to be time-symmetric, so that the association rate of the same set of pairs is given by $A(t) = B(-t)$. The average life time distribution $L(t)$ is then given by the convolution product $A(t) * B(t)$, normalized to produce a probability distribution. The first moment of $L(t)$ then defines a mean life time (MLT) τ of pairs:

$$\tau = \int_0^\infty t L(t)\, dt. \tag{3}$$

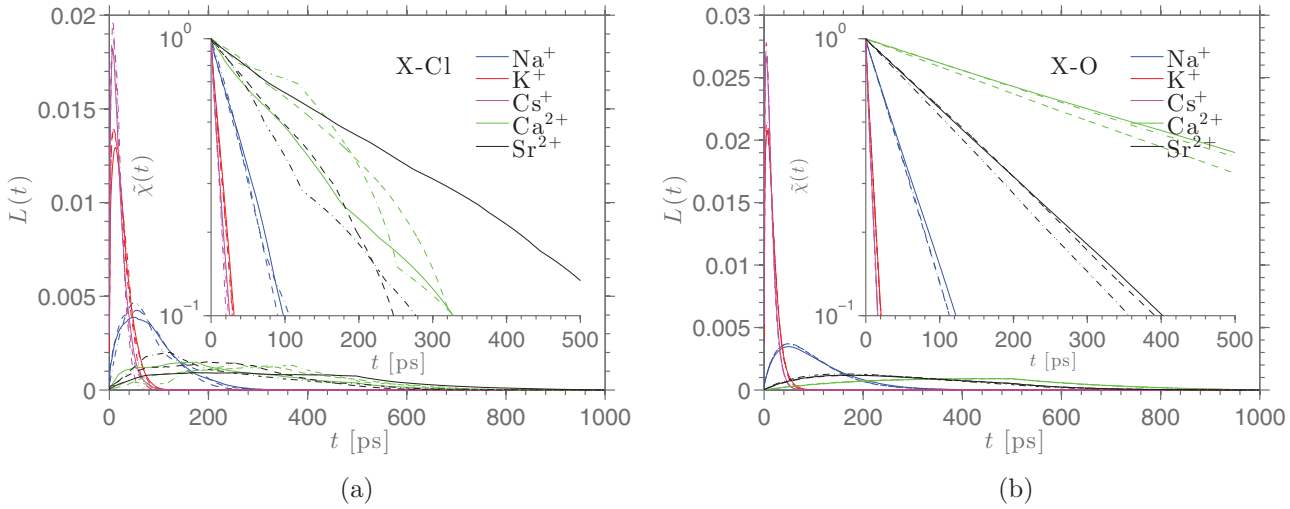

FIG. 9. Life time $L(t)$ functions for the cation-anion (a) and cation-oxygen (b) pairing for the different chloride solutions and concentrations. The dashed-dotted lines correspond to a molar concentration of 0.3 M, the dashed lines to 0.6 M, and the full lines to 0.9 M. The different colors of the lines correspond to the cations species in the chloride solutions: Na^+ (blue), K^+ (red), Cs^+ (magenta), Ca^{2+} (green), and Sr^{2+} (black). The insets in the figures show the corresponding residence functions $\tilde{\chi}(t)$.

Note that the definition of the first moment generally has a normalization term, which we can discard because our life time function is already normalized. The resulting MLT will be twice the MRT value calculated from a function that only represents the forming or breaking of pairs. This definition of the residence time can be applied to a wide range of problems since it does not rely on assumptions about the decay of the correlation function. However, the calculated residence time can become sensitive to the chosen value for the tolerance time as discussed by Laage and Hynes.[9] The residence time is said to be particularly sensitive to the tolerance time when energy barriers are low. This would correspond to situations in which the residence times are short, such that the residence time and the tolerance time become of similar magnitudes. While this could be seen as a weakness of the definition of the residence time, the physical interpretation of the residence time as the "time spent in the first hydration shell" becomes arguable when the hydration shells are not clearly distinguishable anymore (i.e., when the barrier between them flattens).[6]

Figure 9 shows $L(t)$ and $\tilde{\chi}(t)$ for each of the electrolyte solutions. The cation-anion pairs are shown in Figure 9(a) while Figure 9(b) shows pairing between cations and the oxygen atoms of water molecules. The pairing times show reasonable agreement with values reported in the literature,[29,88,99] although a direct quantitative comparison is not possible since the details of the simulations are different. The MLTs are listed in Table S IV in the supplementary material.[47] A weak increase in the MLT is seen as the ion concentration increases, which is consistent with data in the literature.[20] Na^+, Ca^{2+}, and Sr^{2+} (which are kosmotropic) show much longer pairing times (both with water and chloride) than K^+ and Cs^+ (which are chaotropic). This observation is consistent with the separated shells in the corresponding RDFs, which indicate large energy barriers associated with the dissociation of a pair. The ordering in the pairing times of Na^+, K^+, and Cs^+ reveals an inverse proportionality to the ion size. Furthermore, the effect of electrostatic interaction becomes clear from the large pairing times of the bivalent ions. This qualitative relation between charge density and pairing time is simply understood by the fact that the electrostatic interactions with neighbors can be strong if the distance is small or the ion charge large (as explained in Sec. III A). Apart from the ordering of cation-anion or cation-oxygen pairing time, we also find that the cation-anion MLT for K^+ and Cs^+ is greater than the cation-oxygen MLT, while the opposite is true for Na^+, Ca^{2+}, and Sr^{2+}. This qualitatively confirms that the former group of (chaotropic) cations does not favor to be surrounded by water molecules and thus forms ion pairs, while the latter group favors to be surrounded by water. This is consistent with the cation-anion coordination numbers in the inset of Figure 2(a). We furthermore observe that the ions with the shortest pairing life time show the slowest relaxation in the velocity autocorrelation function (Figure S4 in the supplementary material).[47]

The ion-ion residence functions show approximately exponential behavior. This could be explained by the low ion concentration; which causes the ion-ion correlation to exhibit some characteristics of a dilute gas. In a dilute gas, fewer relaxation modes are active, which causes many correlation functions to decay exponentially with time.[98] This argument is not valid for the ion-water correlations and a closer look at the data reveals that the residence functions for K^+ and Cs^+ deviate further from exponential behavior than those for the other ions. This is consistent with the non-exponential short times behavior observed in correlation functions of dense liquids.[98] This indicates a different (possibly inertial) mode of relaxation, that is negligibly short compared to the pairing times of Na^+, Ca^{2+}, and Sr^{2+} but can be more relevant for the other cations. However, we find that the exponential mode still dominates for each of the cations. This is found by rescaling the horizontal and vertical axes of the life time distribution functions by their respective MLT; this gives an almost perfect overlap of the distributions, which implies that the residence functions are described by the same functional form (shown

in Figure S5 in the supplementary material).[47] This could be the case if multiple modes appear at a fixed ratio, but more likely is a scenario in which a single (exponential) mode dominates. It is important to note that our definition of the MLT can be applied without loss of physical significance to other problems, such as the MLT of hydrogen bonds, for which correlation functions show a non-exponential decay.[75,79,83]

C. Shear viscosity

Water is incredibly viscous compared to other solvents with a comparable molar mass.[100] This is mainly assigned to the large amount of structure and hydrogen bonding in water. Structure making ions are expected to increase the shear viscosity while structure breakers should decrease it. The diffusion coefficients in Sec. IV A showed that only structure making behavior is observed in our simulations. This is in agreement with the data by Kim *et al.*,[21] who compared experimentally measured self-diffusion coefficients and shear viscosities to those calculated computationally. The authors found that each of the computational water models considered predicted structure making behavior for electrolytes which are experimentally shown to be structure makers. Other simulation studies also predominantly show decreasing self-diffusion and increasing viscosity with increasing ion concentrations.[20,101] Figure 10 shows the shear viscosities of the aqueous electrolytes. The viscosities are calculated via the Green-Kubo formalism containing the pressure-autocorrelation (PACF) function:

$$\eta = \lim_{t_{max}\to\infty} \frac{V}{k_B T} \int_0^{t_{max}} \langle P_{xy}(t) P_{xy}(0) \rangle \, dt \,, \tag{4}$$

where t_{max} should be chosen large enough such that the PACF has decayed multiple order of magnitude with respect to its initial value. The PACF is shown in Figure S6 in the supplementary material.[47] The shear stress P_{xy} is calculated every 5 fs and the integral is evaluated until $t_{max} = 5$ ps. The decay of the PACF is much slower than that of the velocity-autocorrelation function (which decays to zero in approximately 1 ps), so that the viscosity calculation is much more computationally expensive. The maximum standard error of the data in Figure 10 is 0.05 mPa s (error bars are not shown in the figure for the sake of visibility). Table S V in the supplementary material[47] shows the viscosity values as well as their standard errors. Note that instead of the Green-Kubo formalism, one could calculate the non-equilibrium shear viscosity by applying a constant shear rate to the fluid and calculating the resulting shear stress. Extrapolating these results to a sufficiently small shear rate results in the limiting case of the equilibrium shear viscosity.[102,103] Figure 10 shows that the shear viscosity increases with increasing ion concentration for each electrolyte, but the least for the chaotropic ions (K^+ and Cs^+). These increasing trends with ion concentration confirm the structure making behavior of the different electrolytes considered in this work. Note that the molarity refers to the number of anions in the system, whereas the number of cations depends on their valency (as explained in Sec. II). Thus, the shear viscosities of the solutions with bivalent cations increase stronger with increasing salt concentration than that of the solutions with monovalent cations (despite a smaller number of cations being present in the system). On the other hand, while fewer bivalent cations are present, they mostly occur in a dissociated state, as shown in our previous results. Dissociation is preferable due to the fact that the small bivalent cations interact stronger with water than with chloride ions. This strong electrostatic interaction creates a structured and stable (long life time) hydration shell, which increases the shear viscosity of the electrolyte solution.

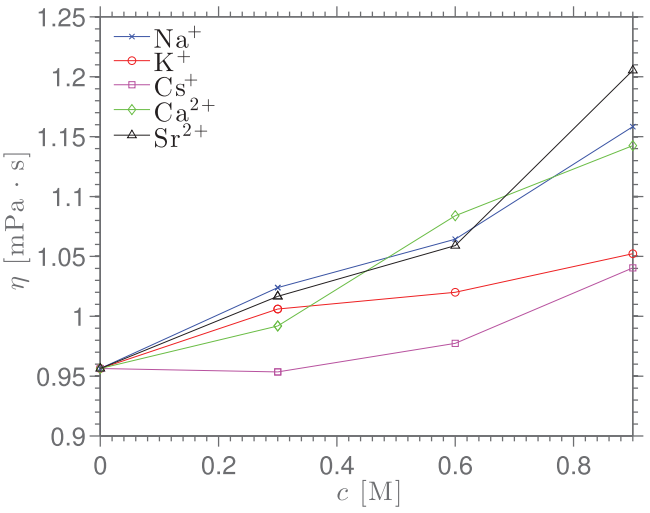

FIG. 10. Shear viscosity for the aqueous electrolytes. The legend indicates the cations while the anion for all simulations is Cl^-. The uncertainties in the data are not shown for the sake of visibility. The maximum standard error of the data is 0.05 mPa s. The different colors of the lines correspond to the cations species in the chloride solutions: Na^+ (blue), K^+ (red), Cs^+ (magenta), Ca^{2+} (green), and Sr^{2+} (black).

V. CONCLUSIONS

Molecular simulations have been used to study the structure and dynamics of conventional and radioactive aqueous electrolytes. Chloride (Cl^-) solutions with five different cations (Na^+, K^+, Cs^+, Ca^{2+}, and Sr^{2+}) at three different ion concentrations (0.3M, 0.6M, and 0.9M) have been compared with the intention to identify the differences between the electrolytes and to study the effect of ion concentration on structure and dynamics. The selection of ions was based on addressing the problems of radioactive waste in (sea)water, and the fact that biological systems often mistake Cs^+ for K^+ and Sr^{2+} for Ca^{2+}.

Overall, the structural differences between K^+ and Cs^+ and between Ca^{2+} and Sr^{2+} are very small. The former ions are chaotropic and interact weakly with surrounding water molecules due to small electric charge and a relatively large ion size. This result is consistent with the description given by Chandler[104] in terms of the solvation free energy. On the other hand, $Ca^{2+}$and Sr^{2+} are kosmotropic, small, and bivalent. These ions form a strong hydration shell, which in turn strongly affects their transport properties. We have shown that the hydration shells around the different cations are kept together in different ways. The hydration shells around $Ca^{2+}$and Sr^{2+} are held together by strong electrostatic forces. The

combination of their bivalent charge and small diameters result in a small dense hydration shell. The rotational freedom of water molecules in the first hydration shell is limited, which prohibits many of the oxygen atoms of these molecules to form hydrogen bonds with other water molecules. On the other hand, K^+ and Cs^+ have weaker electrostatic interactions with surrounding water molecules. This allows the water molecules more freedom to be oriented in such a way that more of the oxygen atoms in the first hydration shell can form hydrogen bonds with water molecules in the second hydration shell. Na^+ behaves mostly similar to the bivalent ions, owing to the fact that this small monovalent ion also has a relatively large charge density. However, we found that the water molecules in the hydration shell around Na^+ can form hydrogen bonds with other water molecules in the same shell, which is not the case for any of the other cations studied here.

The self-diffusion coefficients of ions and water molecules were calculated, as well as the ion-ion and ion-water pairing times and the shear viscosity. The diffusion and viscosity showed a self-consistent picture of structure-making behavior for all ions. K^+ and Cs^+ affect the transport properties less than the other ions. We proposed a formulation for the MLT of a pair. This formalism is easy to apply and not based on an assumption about the functional form of a correlation function. Therefore, it contains its true physical interpretation as the average life time of a pair, regardless of the problem at hand.

Our results are consistent with the conclusions drawn by Fennell *et al.*[1] for monovalent ions. First, large ions of opposite charge tend to associate with each other, despite the weak electrostatic interaction between them. This is a consequence of the fact that these ions have weak interactions with water. The ion pair is held together by a cage of water molecules which holds for a short period of time. Second, pairing between small cations and large anions is not favorable, as seen by the small ion-ion coordination numbers. We extended these conclusions further by investigating the role of ion valence. It was found that $Ca^{2+}$and Sr^{2+} rarely form pairs with Cl^-. This can be explained by the same argument why small cations and large anions dissociate; the interactions between the cation and the nearby water molecules are stronger than the ion-ion interaction. Collins[3] ordered possible combinations between monovalent *kosmotropes* and *chaotropes* based on the interaction strengths. This ordering is representative of the affinity to form ion-ion pairs. Our data show that the order suggested by Collins remains valid for bivalent ions if the terms of *kosmotropes* and *chaotropes* are interpreted as ions with a large and small charge density, respectively.

The confusions in nature between Cs^+ and K^+ and also between Sr^{2+} and Ca^{2+} are understandable, based on each of the structural and dynamic properties studied in this paper. Regardless, a few small differences were observed. The difference in decay of the velocity-autocorrelation functions of K^+ and Cs^+ indicates that the large (more than a factor 3) difference in mass (and thus inertia) could maybe be used to separate these similar cations. The same is true for Sr^{2+} and Ca^{2+}, where the atomic mass of Sr^{2+} is more than twice that of Ca^{2+}. Furthermore, Sr^{2+} and Ca^{2+} show a different coordination number per surface area. This difference could perhaps be used to separate these ions selectively. It would be easier (but not always desirable) to remove ions non-selectively. This can be done in a bulk liquid using, for example, plutonium uranium redox extraction (PUREX),[105] hydrogels,[33,106] or algae.[107,108] However, the typically small concentrations of contaminants make these approaches very inefficient. Furthermore, they tend to be more suitable for removing chaotropic ions than kosmotropic ones (such as strontium). Microporous materials, such as a zeolite or clays, can also be used to remove contaminant in a slightly more selective manner.[35,109,110] Regardless, the need for improving such materials and finding more efficient and selective approaches remains.

ACKNOWLEDGMENTS

This work has been funded by the French region Languedoc-Roussillon through the program "Chercheurs d'Avenir."

[1] C. J. Fennell, A. Bizjak, V. Vlachy, and K. A. Dill, J. Phys. Chem. B **113**, 6782 (2009).
[2] J. Lee, *Concise Inorganic Chemistry*, 5th ed. (Wiley India Pvt. Limited, 2008).
[3] K. D. Collins, Biophys. J. **72**, 65 (1997).
[4] P. Ben Ishai, E. Mamontov, J. D. Nickels, and A. P. Sokolov, J. Phys. Chem. B **117**, 7724 (2013).
[5] A. P. Lyubartsev, K. Laasonen, and A. Laaksonen, J. Chem. Phys. **114**, 3120 (2001).
[6] C. F. Schwenk, T. S. Hofer, and B. M. Rode, J. Phys. Chem. A **108**, 1509 (2004).
[7] Y. Marcus, Chem. Rev. **109**, 1346 (2009).
[8] R. W. Impey, P. A. Madden, and I. R. McDonald, J. Phys. Chem. **87**, 5071 (1983).
[9] D. Laage and J. T. Hynes, J. Phys. Chem. B Lett. **112**, 7697 (2008).
[10] I. S. Joung and T. E. Cheatham, J. Phys. Chem. B **113**, 13279 (2009).
[11] G. Stirnemann, J. T. Hynes, and D. Laage, J. Phys. Chem. B **114**, 3052 (2010).
[12] P.-A. Cazade, R. Hartkamp, and B. Coasne, J. Phys. Chem. C **118**, 5061 (2014).
[13] P. Levitz, P. A. Bonnaud, P.-A. Cazade, R. J.-M. Pellenq, and B. Coasne, Soft Matter **9**, 8654 (2013).
[14] D. Laage and J. T. Hynes, Science **311**, 832 (2006).
[15] D. Laage and J. T. Hynes, Proc. Natl. Acad. Sci. U. S. A. **104**, 11167 (2007).
[16] D. Laage, G. Stirnemann, and J. T. Hynes, J. Phys. Chem. B **113**, 2428 (2009).
[17] D. Laage and J. T. Hynes, J. Phys. Chem. B **112**, 14230 (2008).
[18] D. Laage and J. T. Hynes, Chem. Phys. Lett. **433**, 80 (2006).
[19] S. Tazi, A. Botan, M. Salanne, V. Marry, P. Turq, and B. Rotenberg, J. Phys.: Condens. Matter **24**, 284117 (2012).
[20] H. Du, J. C. Rasaiah, and J. D. Miller, J. Phys. Chem. B **111**, 209 (2007).
[21] J. S. Kim, Z. Wu, A. R. Morrow, A. Yethiraj, and A. Yethiraj, J. Phys. Chem. B **116**, 12007 (2012).
[22] Y. Zhu, S. Ogano, G. Kelsall, and H. A. Spikes, Tribol. Trans. **43**, 175 (2000).
[23] J. C. T. Eijkel and A. van den Berg, Chem. Soc. Rev. **39**, 957 (2010).
[24] A. Siria, P. Poncharal, A.-L. Biance, R. Fulcrand, X. Blase, S. T. Purcell, and L. Bocquet, Nature **494**, 455 (2013).
[25] E. Królak and J. Karwowska, Pol. J. Environ. Stud. **19**, 599 (2010).
[26] Z. Franic and G. Marovic, J. Environ. Radioactiv. **94**, 75 (2007).
[27] R. L. Radtke, Comp. Biochem. Phys. A **92**, 189 (1989).
[28] P. Smirnov and V. Trostin, Russ. J. Gen. Chem. **81**, 282 (2011).
[29] L. M. Hamm, A. F. Wallace, and P. M. Dove, J. Phys. Chem. B **114**, 10488 (2010).
[30] L. X. Dang, X. Sun, B. Ginovska-Pangovska, H. V. R. Annapureddy, and T. B. Truong, Faraday Discuss. **160**, 151 (2013).
[31] B. Jagoda-Cwiklik, R. Vacha, M. Lund, M. Srebro, and P. Jungwirth, J. Phys. Chem. B **111**, 14077 (2007).

[32]V. Kolombet and A. Frolov, Russ. J. Phys. Chem. B **4**, 875 (2010).
[33]D. Deli, K. Law, Z. Liu, D. J. Crouch, F. R. Livens, and S. G. Yeates, React. Funct. Polym. **72**, 414 (2012).
[34]M. Attallah, E. Borai, R. Harjula, A. Paajanen, M. Karesoja, and R. Koivula, J. Mater. Sci. Eng. B **1**, 736 (2011).
[35]J. L. Mertz, Z. H. Fard, C. D. Malliakas, M. J. Manos, and M. G. Kanatzidis, Chem. Mater. **25**, 2116 (2013).
[36]S. Koneshan, J. C. Rasaiah, R. M. Lynden-Bell, and S. H. Lee, J. Phys. Chem. B **102**, 4193 (1998).
[37]S. T. Cui and J. G. Harris, J. Phys. Chem. **99**, 2900 (1995).
[38]S. Smith and B. Kennedy, Geochim. Cosmochim. Acta **47**, 503 (1983).
[39]J. L. F. Abascal and C. Vega, J. Chem. Phys. **123**, 234505 (2005).
[40]C. Vega, J. L. F. Abascal, and I. Nezbeda, J. Chem. Phys. **125**, 034503 (2006).
[41]A. P. Markesteijn, R. Hartkamp, S. Luding, and J. Westerweel, J. Chem. Phys. **136**, 134104 (2012).
[42]D. Rozmanov and P. G. Kusalik, J. Chem. Phys. **136**, 044507 (2012).
[43]P. A. Cazade, J. Dweik, B. Coasne, F. Henn, and J. Palmeri, J. Phys. Chem. C **114**, 12245 (2010).
[44]L. X. Dang, J. Am. Chem. Soc. **117**, 6954 (1995).
[45]L. X. Dang, Chem. Phys. Lett. **227**, 211 (1994).
[46]S. Mamatkulov, M. Fyta, and R. R. Netz, J. Chem. Phys. **138**, 024505 (2013).
[47]See supplementary material at http://dx.doi.org/10.1063/1.4896380 for additional figures and tables to support the results presented in this paper.
[48]F. Moucka, M. Lisal, and W. R. Smith, J. Phys. Chem. B **116**, 5468 (2012).
[49]J. L. Aragones, M. Rovere, C. Vega, and P. Gallo, J. Phys. Chem. B **118**, 7680 (2014).
[50]M. Kohagen, P. E. Mason, and P. Jungwirth, J. Phys. Chem. B **118**, 7902 (2014).
[51]J. Heyda, J. C. Vincent, D. J. Tobias, J. Dzubiella, and P. Jungwirth, J. Phys. Chem. B **114**, 1213 (2010).
[52]G. Lee Warren and S. Patel, J. Chem. Phys. **127**, 064509 (2007).
[53]D. Spangberg and K. Hermansson, J. Chem. Phys. **120**, 4829 (2004).
[54]D. E. Smith and L. X. Dang, J. Phys. Chem. **100**, 3757 (1994).
[55]J. Sala, E. Guardia, and J. Marti, J. Chem. Phys. **132**, 214505 (2010).
[56]T. Weinhart, R. Hartkamp, A. R. Thornton, and S. Luding, Phys. Fluids **25**, 070605 (2013).
[57]F. Goncu, O. Duran, and S. Luding, C. R. Mecanique **338**, 570 (2010).
[58]B. J. Alder, D. M. Gass, and T. E. Wainwright, J. Chem. Phys. **53**, 3813 (1970).
[59]I. S. Joung and T. E. Cheatham, J. Phys. Chem. B **112**, 9020 (2008).
[60]J. L. Aragones, E. Sanz, and C. Vega, J. Chem. Phys. **136**, 244508 (2012).
[61]R. W. Hockney and J. W. Eastwood, *Computer Simulation using Particles* (Taylor and Francis, Inc., Bristol, PA, USA, 1988).
[62]W. G. Hoover, Phys. Rev. A **31**, 1695 (1985).
[63]M. Lund, B. Jagoda-Cwiklik, C. E. Woodward, R. Vacha, and P. Jungwirth, J. Phys. Chem. Lett. **1**, 300 (2010).
[64]K. D. Collins, G. W. Neilson, and J. E. Enderby, Biophys. Chem. **128**, 95 (2007).
[65]E. Wernersson and P. Jungwirth, J. Chem. Theory Comput. **6**, 3233 (2010).
[66]A. Luzar and D. Chandler, Nature **379**, 55 (1996).
[67]A. Luzar, J. Chem. Phys. **113**, 10663 (2000).
[68]J. Marti, J. A. Padro, and E. Guardia, J. Chem. Phys. **105**, 639 (1996).
[69]C. D. Cappa, J. D. Smith, K. R. Wilson, B. M. Messer, M. K. Gilles, R. C. Cohen, and R. J. Saykally, J. Phys. Chem. B **109**, 7046 (2005).
[70]D. Xenides, B. Randolf, and B. Rode, J. Mol. Liq. **123**, 61 (2006).
[71]C. Liu, W. Li, and W. Wang, Phys. Rev. E **87**, 052309 (2013).
[72]A. Malani and K. G. Ayappa, J. Chem. Phys. **136**, 194701 (2012).
[73]H. S. Frank and W.-Y. Wen, Discuss. Faraday Soc. **24**, 133 (1957).
[74]A. W. Omta, M. F. Kropman, S. Woutersen, and H. J. Bakker, Science **301**, 347 (2003).
[75]A. Luzar and D. Chandler, Phys. Rev. Lett. **76**, 928 (1996).
[76]F. G. Alabarse, J. Haines, O. Cambon, C. Levelut, D. Bourgogne, A. Haidoux, D. Granier, and B. Coasne, Phys. Rev. Lett. **109**, 035701 (2012).
[77]A. D. Hammerich and V. Buch, J. Chem. Phys. **128**, 111101 (2008).
[78]J. D. Smith, C. D. Cappa, K. R. Wilson, R. C. Cohen, P. L. Geissler, and R. J. Saykally, Proc. Natl. Acad. Sci. U. S. A. **102**, 14171 (2005).
[79]R. Kumar, J. R. Schmidt, and J. L. Skinner, J. Chem. Phys. **126**, 204107 (2007).
[80]D. Swiatla-Wojcik, Chem. Phys. **342**, 260 (2007).
[81]D. Prada-Gracia, R. Shevchuk, and F. Rao, J. Chem. Phys. **139**, 084501 (2013).
[82]A. Nag, D. Chakraborty, and A. Chandra, J. Chem. Sci. **120**, 71 (2008).
[83]A. Chandra, Phys. Rev. Lett. **85**, 768 (2000).
[84]B. Hribar, N. T. Southall, V. Vlachy, and K. A. Dill, J. Am. Chem. Soc. **124**, 12302 (2002).
[85]E. Guardia, D. Laria, and J. Marti, J. Phys. Chem. B **110**, 6332 (2006).
[86]S. H. Lee and J. C. Rasaiah, J. Chem. Phys. **101**, 6964 (1994).
[87]A. K. Soper and K. Weckstrom, Biophys. Chem. **124**, 180 (2006).
[88]T. Peng, T.-M. Chang, X. Sun, A. V. Nguyen, and L. X. Dang, J. Mol. Liq. **173**, 47 (2012).
[89]S. R. Varanasi, P. Kumar, and Y. Subramanian, J. Chem. Phys. **137**, 144506 (2012).
[90]K. Meier, A. Laesecke, and S. Kabelac, J. Chem. Phys. **121**, 9526 (2004).
[91]H. Chakrabarti, Phys. Rev. B **51**, 12809 (1995).
[92]R. Mills and V. Lobo, *Self-diffusion in Electrolyte Solutions: A Critical Examination of Data Compiled from the Literature*, Physical Sciences Data, Vol. 36 (Elsevier, 1989).
[93]B. M. Braun and H. Weingaertner, J. Phys. Chem. **92**, 1342 (1988).
[94]J. Walter, S. Deublein, S. Reiser, M. Horsch, J. Vrabec, and H. Hasse (Springer, Berlin/Heidelberg, 2012).
[95]Y. Ding, A. A. Hassanali, and M. Parrinello, Proc. Natl. Acad. Sci. U. S. A. **111**, 3310 (2014).
[96]R. Hartkamp, S. Bernardi, and B. D. Todd, J. Chem. Phys. **136**, 064105 (2012).
[97]J. C. Rasaiah and R. Lynden-Bell, Philos. Trans. R. Soc. London, Ser. A **359**, 1545 (2001).
[98]R. Hartkamp, P. J. Daivis, and B. D. Todd, Phys. Rev. E **87**, 032155 (2013).
[99]S. Deublein, S. Reiser, J. Vrabec, and H. Hasse, J. Phys. Chem. B **116**, 5448 (2012).
[100]J. O. M. Bockris and A. K. N. Reddy, *Modern Electrochemistry: An Introduction to an Interdisciplinary Area* (Plenum Press, New York, 1977), Vol. 1.
[101]D. A. Turton, J. Hunger, G. Hefter, R. Buchner, and K. Wynne, J. Chem. Phys. **128**, 161102 (2008).
[102]J. Delhommelle and J. Petravic, J. Chem. Phys. **118**, 2783 (2003).
[103]R. Hartkamp, B. D. Todd, and S. Luding, J. Chem. Phys **138**, 244508 (2013).
[104]D. Chandler, Nature **437**, 640 (2005).
[105]G. R. Choppin, J.-O. Liljenzin, and J. Rydberg, *Radiochemistry and Nuclear Chemistry*, 3rd ed. (Butterworth-Heinemann, 1995).
[106]H. A. Shawky, M. H. El-Sayed, A. E.-H. Ali, and M. S. Abdel Mottaleb, J. Appl. Polym. Sci. **100**, 3966 (2006).
[107]S. K. Mehta and J. P. Gaur, Crit. Rev. Biotechnol. **25**, 113 (2005).
[108]M. Kalin, W. Wheeler, and G. Meinrath, J. Environ. Radioact. **78**, 151 (2004).
[109]P. Weisz, Chem. Technol. **3**, 498 (1973).
[110]A. Sachse, A. Merceille, Y. Barré, A. Grandjean, F. Fajula, and A. Galarneau, Microporous Mesoporous Mater. **164**, 251 (2012).